

Forecasting the Forced van der Pol Equation with Frequent Phase Shifts Using Reservoir Computing

Sho Kuno^{1, a)} and Hiroshi Kori^{1, 2, b)}

¹⁾Department of Mathematical Informatics, The University of Tokyo, Tokyo 113-8656, Japan.

²⁾Department of Complexity Sciences and Engineering, The University of Tokyo, Kashiwa, Chiba 277-8561, Japan.

(Dated: 2 July 2024)

We tested the performance of reservoir computing (RC) in predicting the dynamics of a certain non-autonomous dynamical system. Specifically, we considered a van der Pol oscillator subjected to periodic external force with frequent phase shifts. The reservoir computer, which was trained and optimized with simulation data generated for a particular phase shift, was designed to predict the oscillation dynamics under periodic external forces with different phase shifts. The results suggest that if the training data have some complexity, it is possible to quantitatively predict the oscillation dynamics exposed to different phase shifts. The setting of this study was motivated by the problem of predicting the state of the circadian rhythm of shift workers and designing a better shift work schedule for each individual. Our results suggest that RC could be exploited for such applications.

Shift workers who regularly shift their sleep-wake schedules are known to have increased risk of various diseases, and circadian rhythm disturbances are thought to be an important risk factor. The behavior of circadian rhythms exposed to light-dark cycles is commonly modeled as a non-autonomous system, namely, a limit-cycle oscillator subjected to external periodic forces. Suppose that a shift worker can choose to change from one shift work schedule to another. If the dynamics of the circadian rhythm under the new schedule can be predicted in advance, this information can be used to make a scheduling decision. Mathematical modeling is a tool that makes this determination possible. However, it is difficult to construct reliable mathematical models precisely reproducing actual dynamics. Moreover, it is difficult to obtain optimized parameters for each individual from limited observational data. Reservoir computing (RC) may provide another solution to this problem. Against this background, this study was conducted to examine whether RC can predict the dynamics of limit cycle oscillators subjected to periodic forces with frequent phase shifts, such as those experienced by shift workers. Our results suggest that RC may potentially contribute to forecasting the circadian rhythms of shift workers.

I. INTRODUCTION

Nonautonomous dynamical systems are dynamical systems whose evolution is determined by time-variant external drives and parameter effects. These systems are responsive to external effects and time-varying conditions. Thus, they are utilized in various fields, such as engineering, physics, biomedical science, ecology, climate, and neuroscience, for modeling various phenomena^{1,2}.

Circadian clock dynamics, a factor in various important academic and societal issues, is typically modeled as a nonautonomous system. The circadian clock is a self-sustained oscillator, which produces daily variations in genetic and physiological activities. Moreover, the clock is approximately synchronized with the light-dark (LD) cycle of the environmental day-night rhythms, with a period of 24 h. Recently, the effect of jet lag and shift work on the circadian clock has attracted considerable research attention, because these effects are thought to have a significant impact on human health³⁻⁵. The circadian clock is often modeled as a limit-cycle oscillator subjected to external periodic driving⁶⁻⁹. By exploiting a mathematical model, we may anticipate the effect of a phase shift to the LD cycle on the circadian clock. However, it is challenging to construct a reliable model and infer the model parameters to fit real data.

Recent data-driven trends in machine learning may offer alternative approaches to address this issue. Recurrent neural networks (RNNs), a framework of artificial neural networks (ANNs), are particularly suited for problems originating from dynamical systems. They exploit the past information along with the present to update their hidden states, enabling them to capture the temporal dependencies of the sequential data. In particular, the long short-term memory (LSTM) RNN subtype succeeds in addressing the long-term dependency problem and achieves better precision¹⁰⁻¹⁴. Despite its success in the learning tasks of dynamical systems, LSTM has the

^{a)}Electronic mail: kunoshota1225@g.ecc.u-tokyo.ac.jp

^{b)}Electronic mail: kori@k.u-tokyo.ac.jp

drawback of long computing time. A traditional challenge of designing these RNN schemes is achieving a better tradeoff balance of the prediction precision and the computational cost of the training algorithms.

Reservoir Computing (RC), or echo-state network, is an innovative framework for RNNs that combines high fidelity in replicating dynamics and efficiency in computation. In RC, the input and hidden layers are initialized with randomly selected matrices, and only the read-out layer requires training¹⁵. Further, RC requires only a linear regression for fitting, and no back-propagation that involves nonlinear computation is necessary. Despite this simple structure that distinguishes RC from previous RNN frameworks, RC is remarkably effective for dynamical-systems learning tasks even for chaotic systems^{16–20}, whose sensitive dependence on initial conditions makes the prediction task more daunting. Moreover, data driven approaches on learning tasks of partially or sparse observed systems have carefully been inspected^{21–27}.

RC has been tested for learning tasks of nonautonomous dynamical systems as well. Prominent research was reported in Ref. 28, where the authors used RC to predict the future state of various chaotic systems with external drives. Specifically, they employed a sinusoidal function with a slowly growing amplitude as an external drive. It was demonstrated that RC can successfully predict the system's behavior if the external drive is known. This scenario is similar to the problem of predicting a shift worker's biological clock. In the case of shift workers, if they are exposed to light during waking hours and darkness during sleeping hours, the external drive corresponding to shift work is known. However, unlike the scenario described in Ref. 28, the external drive involves frequent and abrupt phase shifts corresponding to changes in working hours. It is necessary to investigate whether RC can accurately predict dynamics even for external drives with such phase shifts.

Therefore, in this study, we asked whether RC can predict the dynamics of limit-cycle oscillators subjected to an external drive with frequent and abrupt phase shifts. Data were generated by a simple model: We employed the van der Pol equation as a limit-cycle oscillator and modeled the external drive is a sinusoidal function. We found that RC can indeed precisely predict oscillation dynamics under certain situations.

This paper is organized as follows: Section II explains the methods used for our experiments and the results. Section III presents the conclusion, followed by a discussion of the results and possible applications, focusing on the circadian rhythm.

II. METHOD AND RESULTS

We assumed that a person who has experienced a certain schedule of shift working will at some point change to a new, different schedule. Our aim was to forecast

the dynamics of the circadian clock for the new schedule on the basis of past data and the new schedule. Our concrete procedure is described here.

A. Model and Simulation

We used the forced van der Pol model with an external drive $P_n(t)$, expressed as

$$\frac{dv}{dt} = w, \quad (1a)$$

$$\frac{dw}{dt} = \mu(1 - v^2)w - v + P_n(t). \quad (1b)$$

For $P_n(t)$, we chose the following sinusoidal function with a phase shift function $\theta_n(t)$:

$$P_n(t) := A \sin(\Omega t + \theta_n(t)), \quad (2a)$$

$$\theta_n(t) := \frac{n}{24} \left\lfloor \frac{t}{4T_e} \right\rfloor 2\pi. \quad (2b)$$

where A and Ω are the strength and frequency of the external drive, respectively, and $T_e := \frac{2\pi}{\Omega}$ is the period of the external drive in the absence of phase shifts. The external drive is a model of the day-night rhythm in the context of the circadian clock system; we thus interpreted T_e as one day (1 d). The function $\theta_n(t)$ shifts the phase of $P_n(t)$ by n hours every 4 d, with $n \in \mathbb{Z}$, $-12 \leq n \leq 12$.

Our numerical simulations were conducted using the `scipy.integrate.solve_ivp` package in Python. Time series were sampled with a time step $h := \frac{T_e}{M}$, where $M = 100$ is the number of divisions. To avoid inconveniences caused by the discontinuity of $P_n(t)$ during the simulation, the data were generated by repeating numerical integrations over the individual intervals between each phase shift and concatenating the obtained time series. Because a phase shift was injected every 4 d, each time series segment had $4M$ time steps.

Throughout the study, we fixed $A = 0.5$ and $\Omega = 1.05$. This choice was motivated by the fact that circadian clocks in mice are considerably disturbed for a phase advancing condition⁵. Figure 1 shows the first 50 d of the data sets (only for the variables $x(t)$ and $P_n(t)$) obtained by a simulation for each $n \in \{-7, 0, 7\}$. The case of $n = 0$ corresponds to the forced van der Pol model without any phase shift to the external drive, whereby the obtained time series is genuinely periodic. For $n = -7$, despite rapid changes in $P_n(t)$, the waveform of $x(t)$ remains nearly periodic. In contrast, for $n = 7$, $x(t)$ is considerably distorted and seemingly aperiodic. As targeted, the forced van der Pol equation indeed showed weaker, more disrupted oscillations in the forward shifts than the backward ones.

We defined the past schedule of a shift worker as $P_n(t)$ with $n \in \{-7, 0, 7\}$, and the new schedule as

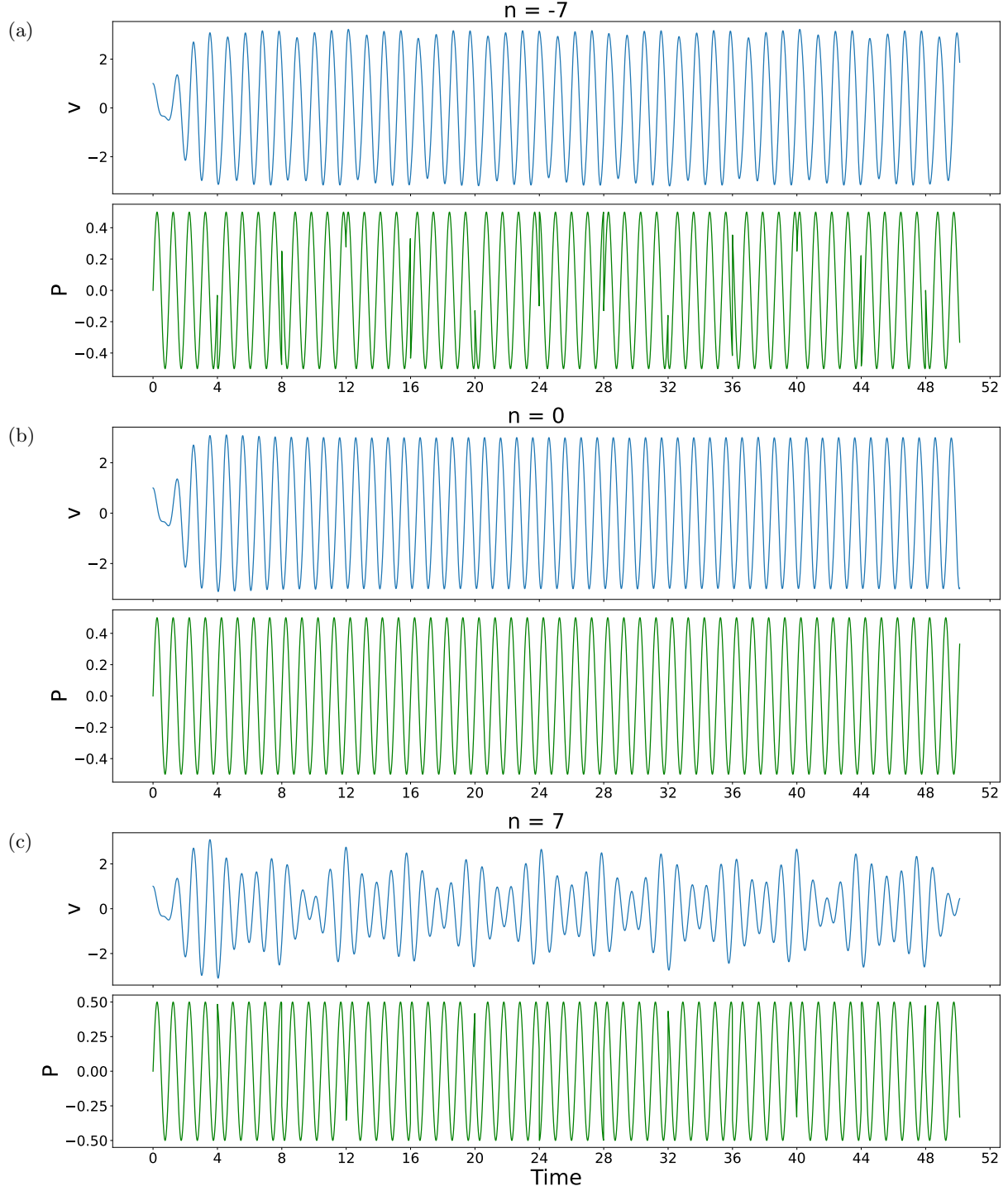


FIG. 1: Variable v of the van der Pol equation subjected to external drive $P_n(t)$, to which the phase shift of n hours is applied at every 4 d. (a) $n = -7$, (b) $n = 0$, and (c) $n = 7$.

$P_m(t)$ with $m \in \{-11, -10, \dots, 12\}$. We thus generated the data sets $\{v_i^{(n)}, w_i^{(n)}, P_i^{(n)}\}$ for $n \in \{-7, 0, 7\}$ and divided them into two consecutive parts: the training and testing periods, denoted as $\{v_{i,\text{train}}^{(n)}, w_{i,\text{train}}^{(n)}, P_{i,\text{train}}^{(n)}\}$

($i = 0, \dots, N_{\text{train}}$) and $\{v_{i,\text{test}}^{(n)}, w_{i,\text{test}}^{(n)}, P_{i,\text{test}}^{(n)}\}$ ($i = 0, \dots, N_{\text{test}}$), respectively. As detailed previously, the former and latter were generated for the RC training and the optimization, respectively. Using the final data as the initial condition, we further gener-

ated the data sets for forecast verification, denoted as $\{v_{i,\text{forecast}}^{(n \rightarrow m)}, w_{i,\text{forecast}}^{(n \rightarrow m)}, P_{i,\text{forecast}}^{(m)}\}$ ($i = 0, \dots, N_{\text{forecast}}$), where $m \in \{-11, -10, \dots, 12\}$. We set $N_{\text{train}} = 8000$, $N_{\text{test}} = 4000$, $N_{\text{forecast}} = 3000$, corresponding to the period of 80 d, 40 d, and 30 d.

B. Reservoir Computer

The structure of our RC is illustrated in Fig. 2. We adopted the basic RC structure described in Ref. 15. The standard RC model consists of three layers: the input, hidden (reservoir), and readout layers. We denoted the data used as the input for updating the reservoir dynamics by $\mathbf{x}_i \in \mathbb{R}^{d_x}$. In the input layer, \mathbf{x}_i is mapped to a hidden variable $\mathbf{r}_i \in \mathbb{R}^{d_r}$ of a much higher dimension $d_r > d_x$ inside the hidden layer by a linear transformation W_{in} of size $d_r \times d_x$:

$$\mathbf{u}_i = W_{\text{in}} \mathbf{x}_i. \quad (3)$$

In the hidden layer, \mathbf{r}_i is updated by a $d_r \times d_r$ linear transformation W_r using an activation function $\tanh(\cdot)$. The updating equation of the reservoir state is defined using a variable α of the leaking rate:

$$\mathbf{r}_{i+1} = (1 - \alpha) \mathbf{r}_i + \alpha \tanh(\mathbf{u}_{i+1} + W_r \mathbf{r}_i), \quad (4)$$

The leaking rate α is a parameter that controls the effectiveness of the past information on reservoir dynamics, which enables it to regulate the length of the memory the RC can store inside. The readout is obtained with another linear transformation W_{out} of size $d_z \times d_r$,

$$\mathbf{y}_i = W_{\text{out}} \mathbf{r}_i. \quad (5)$$

As a main feature of RC, the matrices W_{in} and W_r are both randomly selected matrices of weights before the training, whereas W_{out} is the only part trained to fit the prediction \mathbf{y}_i to \mathbf{x}_i . W_{out} is obtained by solving a least-squares problem of the form

$$W_{\text{out}} := \arg \min_{V \in \mathbb{R}^{d_z \times d_r}} \|X - VR\|_F, \quad (6)$$

where $X = (\mathbf{x}_1 \mathbf{x}_2 \dots \mathbf{x}_{N-1}) \in \mathbb{R}^{d_x \times N-1}$ and $R = (\mathbf{r}_1 \mathbf{r}_2 \dots \mathbf{r}_{N-1}) \in \mathbb{R}^{d_r \times N-1}$. To solve this problem, we employ Tikhonov regularization with a regularity parameter $\lambda \geq 0$, which yields a formal solution of the form

$$W_{\text{out}} := ZR^\top (RR^\top + \lambda I)^{-1}, \quad (7)$$

where I is the identity matrix.

C. Training and Optimization

We used the data sets for $n = -7, 0, +7$ for training and optimizing the reservoir computer. For training, the

input $\mathbf{x}_i = (v_{i,\text{train}}^{(n)}, w_{i,\text{train}}^{(n)}, P_{i,\text{train}}^{(n)})$ was employed. After training, the input $\mathbf{x}_i = (v_{i,\text{test}}^{(n)}, w_{i,\text{test}}^{(n)}, P_{i,\text{test}}^{(n)})$ was employed for optimizing the reservoir computer. Specifically, the RC hyperparameters were tuned to minimize

$$\text{NRMSE} = \sqrt{\frac{\sum_{i=0}^{N_{\text{test}}-1} (\mathbf{x}_i - \mathbf{y}_i)^2}{N_{\text{test}}}}, \quad (8)$$

where $\mathbf{y}_i = (\hat{v}_i^{(n)}, \hat{w}_i^{(n)}, \hat{P}_i^{(n)})$ is the prediction of \mathbf{x}_i by the reservoir computer.

The obtained hyperparameter sets for each case of n are listed in Appendix A. For $n = 7$, the comparison between the input and the prediction is shown in Fig. 3. We observed that the input $v_{i,\text{test}}^{(n)}$ and its prediction $\hat{v}_{i,\text{test}}^{(n)}$, which is the component of \mathbf{y}_i , agree closely. For $n = -7$ and 0, the input and prediction were also nearly indistinguishable (results not shown).

For the RC implementation, we used the `reservoirpy` package in Python²⁹, with another Python library option available, `PyRCN`³⁰. For the optimization process, we used `Optuna`³¹, one of the standard libraries for parameter tuning. Of the several algorithms available for the optimization and pruning processes, we used `optuna.samplers.CmaEsSampler` and `optuna.pruners.SuccessiveHalvingPruner`. `reservoirpy` was designed to be compatible with `hyperopt`³² as well, but its functions may vary from `Optuna`.

D. Forecast

After the RC was trained and optimized for each $n \in \{-7, 0, 7\}$, we conducted the forecasting task. To start forecasting, we “warmed up” the RC with the last insignificant segment in the testing period of \mathbf{x} , contained in the accessible part of the data. Next, we conducted a forecast using the input given by

$$\mathbf{x}_i = (\hat{v}_i, \hat{w}_i, P_{i,\text{forecast}}^{(m)}), \quad (9)$$

where $m \in \{-11, 10, \dots, 12\}$. Note that, whereas the first two elements are those of the prediction \mathbf{y}_i , resulting in an input-output loop, the third element is the true external drive.

An example of the time series of the true and predicted v_i is shown in Fig. 4, where $n = 7$ and $m = 10$; that is, the training and optimization were done using a shift of 7 hours and the forecast was conducted for a shift of 10 hours. As shown in Fig. 5, we quantified the performance of the forecast using the error defined by

$$E^{(n \rightarrow m)} := \log_{10} \sqrt{\frac{\sum_{i=0}^{N_{\text{forecast}}-1} (\hat{v}_i - v_{i,\text{forecast}}^{(n \rightarrow m)})^2}{N_{\text{forecast}}}}. \quad (10)$$

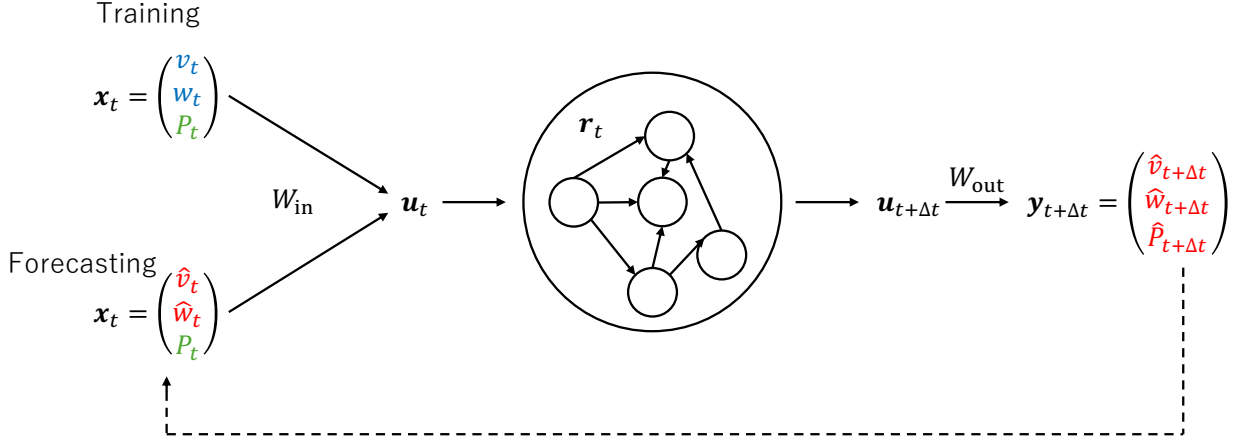


FIG. 2: Basic RC structure. The input x_t is mapped onto u_t in the hidden layer by the matrix W_{in} . During the training and testing periods, the RC is fed with the true data x_t of the dynamical system at every step. During the forecasting phase, the reservoir computer updates autonomously using its output as the input for the new step. Here, we inject the true value of the external drive $P_n(t)$ into the input assuming that $P_n(t)$ is accessible at all times, including the forecast period.

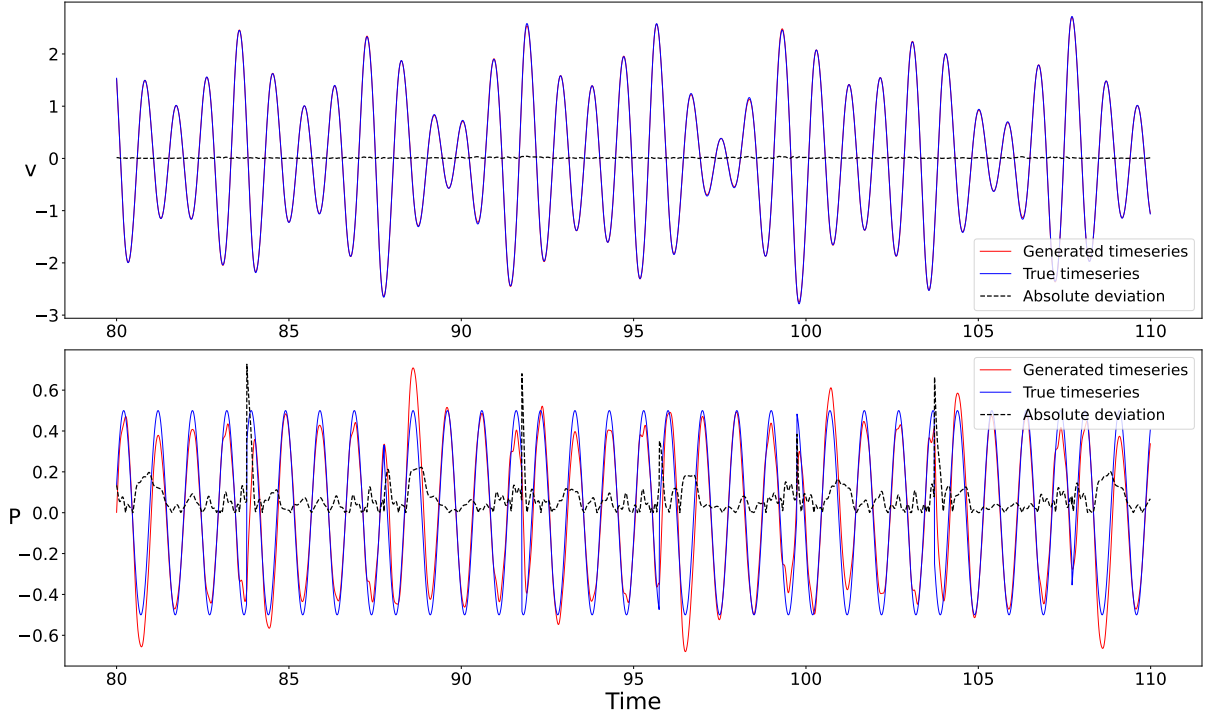


FIG. 3: Prediction by RC of the data with $n = 7$ during the testing period. Only v and $P_n(t)$ are shown.

For the dataset, we prepared two types, one with array $v, w, P_n(t)$ and the other with $v, P_n(t)$. For the first type, the reservoir computer was fed with $x, y, P_n(t)$ during the training and testing phases. For the second, only $x, P_n(t)$ were available during the same phase. In Fig. 6, we show the standard deviation of the generated and true data for each n .

III. CONCLUSION AND DISCUSSION

In this study, we investigated the forecasting ability of RC using the time series of the forced van der Pol equation with frequent phase shifts to its external drive. We tested three different sets of training data shown in Fig. 1; the prediction performance is summarized in Figs. 5 and 6. For $n = 7$, where the training data were com-

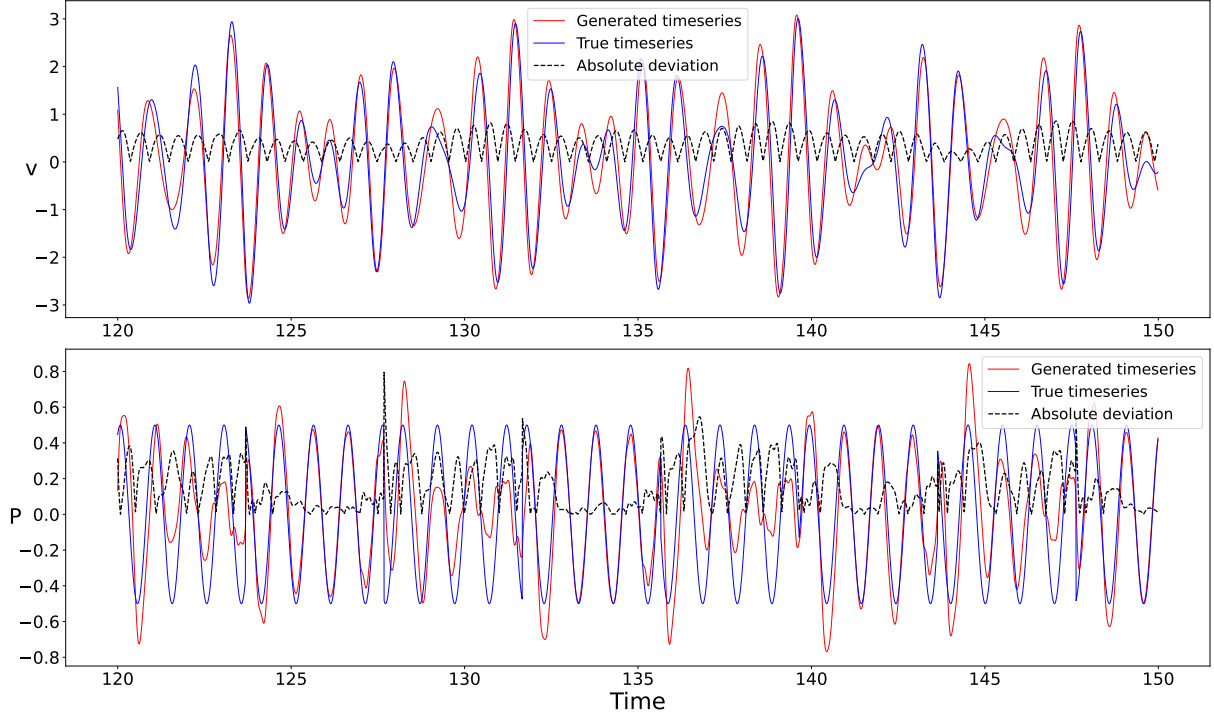


FIG. 4: Time series of the prediction and true v_i for $n = 7$ and $m = 10$ during the forecast period. Only v and $P_n(t)$ are shown.

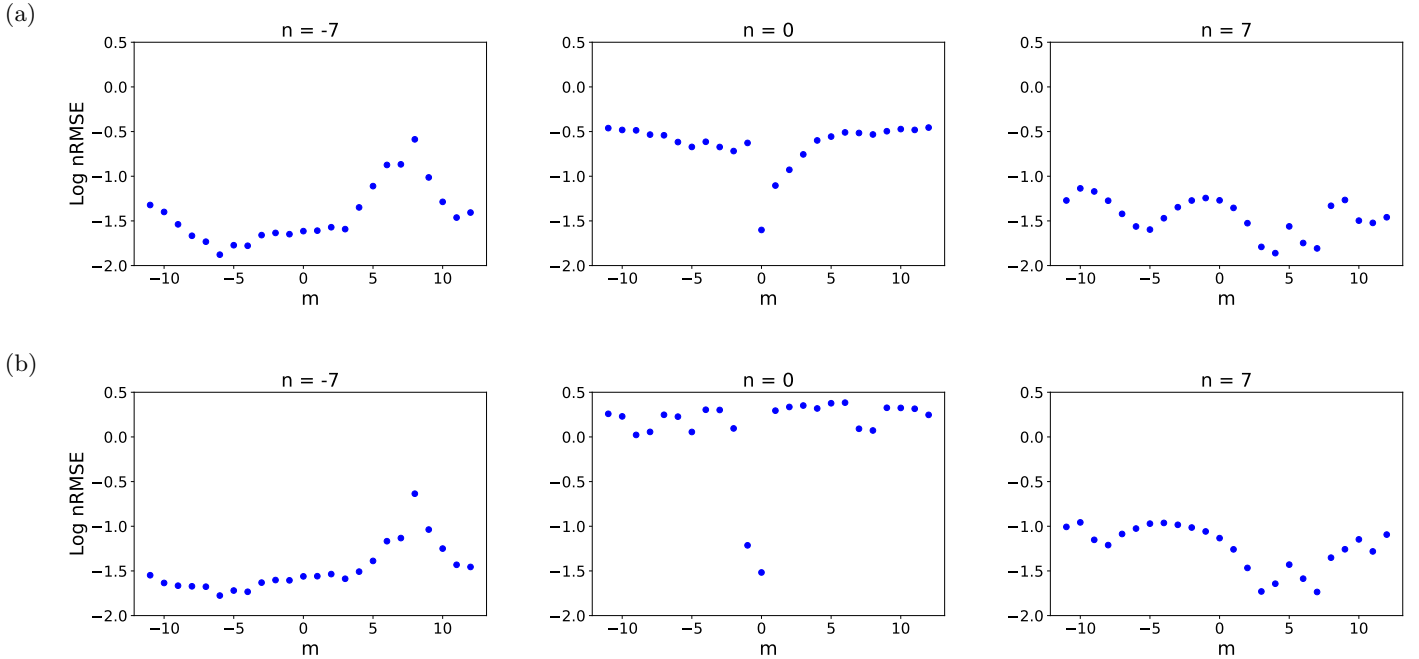


FIG. 5: Error of the forecast, $E^{(n \rightarrow m)}$, for $n = -7, 0, 7$ and $m \in \{-11, 10, \dots, 12\}$, where the input was (a) $\mathbf{x} = (v, w, P_n)$ and (b) $\mathbf{x} = (v, P_n)$.

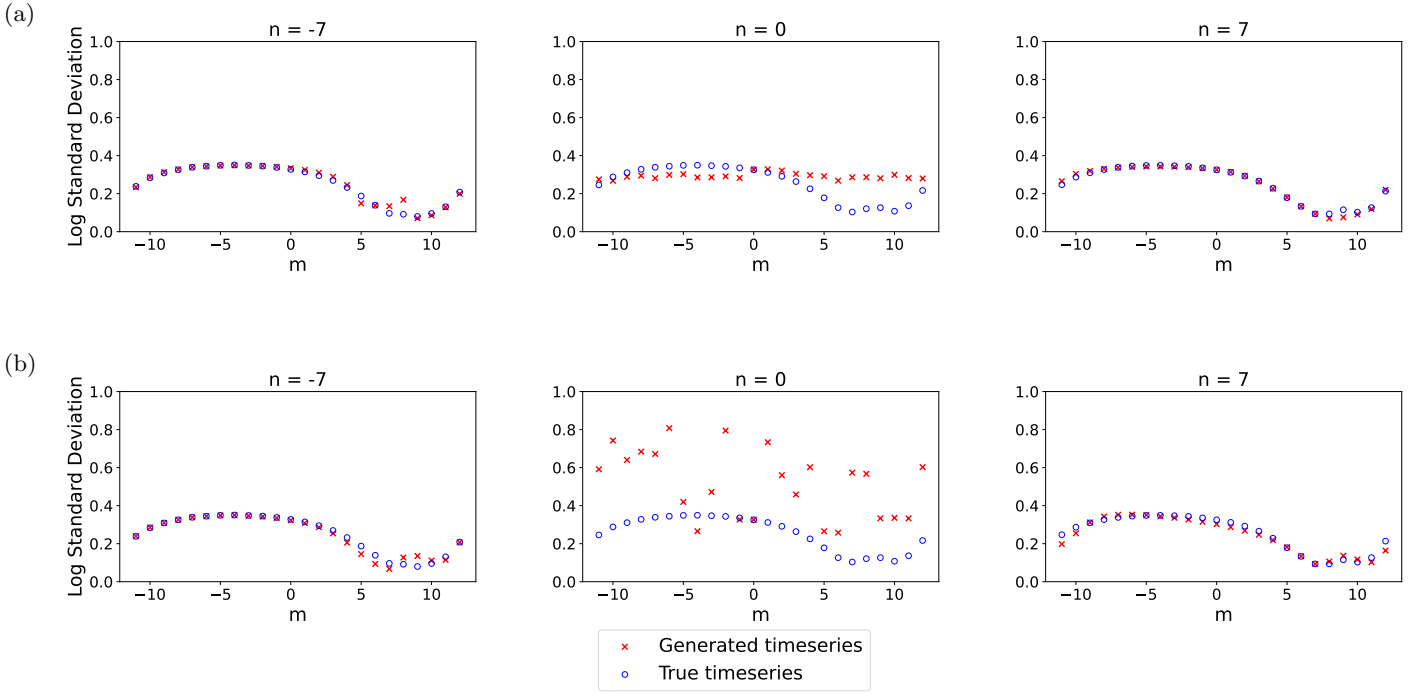


FIG. 6: Standard deviation of the true and generated time series of $v(t)$, where the input was (a) $\mathbf{x} = (v, w, P_n)$ and (b) $\mathbf{x} = (v, P_n)$.

plex (Fig. 1(c)), the predictions were relatively accurate across all values of m . For $n = -7$, in which the training data were not highly complex (Fig. 1(a)), the predictions were generally accurate, though the accuracy degraded for some positive values of m . For $n = 0$, in which the training data were purely periodic (Fig. 1(b)), the overall results were rather poor, except when m was close to $n = 0$. Unsurprisingly, the RC performance was excellent when the target data exhibited a pattern similar to that of the training data. It is remarkable that the reservoir computer, trained using a particular data set (i.e., a particular n value), could predict complex dynamics of different situations (i.e., various m values) unless the training data are too simple. In addition, as shown in Figs. 5(b) and 6(b), the reservoir computer could forecast the future even when only some of the variables were observable. This result is important in applications where the number of observable variables is limited.

Our results are consistent with those of Ref. 28, in which it was demonstrated that RC can accurately forecast chaotic dynamical systems with an external drive that has a slowly growing amplitude. In our study, the setting was distinguished from that of this previous study in that the external drive experienced frequent and rapid phase shifts. It is generally difficult to predict the response of a system to abrupt changes in perturbations. From an application point of view, predictions for such perturbations are important and our results support the usefulness of RC.

Finally, we discuss future studies. As has been noted

throughout this paper, the setting of this study was motivated by the problem of predicting shift workers' circadian rhythms. Our results show that predictions are possible in a practical setting for simulated data from a simple mathematical model. However, the predictive power of the proposed model for data generated by more-complex and possibly stochastic models, and more importantly for real data, needs further exploration.

Although we demonstrated the performance of RC with the most basic structure, various advanced versions and RC algorithms exist; options include the online learning^{33,34} and ensemble methods^{35–37}. The next-generation reservoir computer is another RC scheme that achieves enhanced computational efficiency under certain conditions³⁸.

Theoretical analysis of the prediction of nonautonomous dynamical systems by RC complements our experimental results as well³⁹. Furthermore, RC has been widely studied for aspects of its dimensions⁴⁰ and network structures⁴¹. The relationship between RC and Taken's embedding theorem is indicated to explain the universal approximation of RC^{42–44} as well. Studies on the role of hyperparameters^{45–48} provide practical guides on the selection of hyperparameters in various settings. These theoretical and practical insights into RC could further enhance its performance in learning nonautonomous dynamical systems, potentially leading to broader applications.

ACKNOWLEDGMENTS

This study was supported by JSPS KAKENHI (No. JP21K12056, JP22K18384, JP23K27487) to H.K.

DATA AVAILABILITY STATEMENT

Data available on request from the authors.

Appendix A: Hyperparameters

The set of hyperparameters subjected to optimization explained in [II C](#) are:

- **sr**: the spectral radius of the hidden layer,
- **lr**: leaking rate α that appears in eq. 4.
- **iss**: the input scaling of W_{in} ,
- **ridge**: the ridge value λ of ridge regression.

The search space of the hyperparameters are:

$$\begin{aligned} \text{sr} &\in [10^{-2}, 10], \\ \text{lr} &\in [10^{-9}, 1], \\ \text{iss} &\in [0, 1], \\ \text{ridge} &\in [10^{-9}, 10^{-2}]. \end{aligned}$$

The set of hyperparameters chosen for the result is presented in Table I. We fixed the cell number of RC to 500.

Variables of Data	n	sr	lr	Iss	ridge
$v, P_n(t)$	-7	0.0182	0.0583	0.6833	5.44e-07
$v, P_n(t)$	0	0.6338	0.4487	0.6650	2.40e-04
$v, P_n(t)$	7	0.0696	0.2888	0.3732	4.69e-07
$v, w, P_n(t)$	-7	0.3625	0.0734	0.3330	2.96e-05
$v, w, P_n(t)$	0	0.2420	0.0409	0.6981	3.86e-07
$v, w, P_n(t)$	7	0.0610	0.0242	0.5831	7.67e-03

TABLE I: Hyperparamters in [II C](#).

- ¹S. Strogatz, *Nonlinear Dynamics and Chaos: With Applications to Physics, Biology, Chemistry, and Engineering* (CRC Press, 2018).
- ²J. Guckenheimer and P. Holmes, *Nonlinear Oscillations, Dynamical Systems, and Bifurcations of Vector Fields*, Applied Mathematical Sciences (Springer New York, 2013).
- ³N. M. Kettner, H. Voicu, M. J. Finegold, C. Coarfa, A. Sreekumar, N. Putluri, C. A. Katchy, C. Lee, D. D. Moore, and L. Fu, "Circadian Homeostasis of Liver Metabolism Suppresses Hepatocarcinogenesis," *Cancer Cell* **30**, 909–924 (2016).
- ⁴Y. Yamaguchi and H. Okamura, "Vasopressin Signal Inhibition in Aged Mice Decreases Mortality under Chronic Jet Lag," *iScience* **5**, 118–122 (2018).

- ⁵H. Inokawa, Y. Umemura, A. Shimba, E. Kawakami, N. Koike, Y. Tsuchiya, M. Ohashi, Y. Minami, G. Cui, T. Asahi, R. Ono, Y. Sasawaki, E. Konishi, S.-H. Yoo, Z. Chen, S. Teramukai, K. Ikuta, and K. Yagita, "Chronic circadian misalignment accelerates immune senescence and abbreviates lifespan in mice," *Sci Rep* **10**, 2569 (2020).
- ⁶D. Gonze and A. Goldbeter, "Entrainment Versus Chaos in a Model for a Circadian Oscillator Driven by Light-Dark Cycles," *Journal of Statistical Physics* **101**, 649–663 (2000).
- ⁷G. Kurosawa and A. Goldbeter, "Amplitude of circadian oscillations entrained by 24-h light–dark cycles," *Journal of Theoretical Biology* **242**, 478–488 (2006).
- ⁸H. Kori, Y. Yamaguchi, and H. Okamura, "Accelerating recovery from jet lag: Prediction from a multi-oscillator model and its experimental confirmation in model animals," *Sci Rep* **7**, 46702 (2017).
- ⁹Y. Yamaguchi, T. Suzuki, Y. Mizoro, H. Kori, K. Okada, Y. Chen, J.-M. Fustin, F. Yamazaki, N. Mizuguchi, J. Zhang, X. Dong, G. Tsujimoto, Y. Okuno, M. Doi, and H. Okamura, "Mice genetically deficient in vasopressin V1a and V1b receptors are resistant to jet lag," *Science* **342**, 85–90 (2013).
- ¹⁰N. Mohajerin and S. L. Waslander, "Multistep Prediction of Dynamic Systems With Recurrent Neural Networks," *IEEE Transactions on Neural Networks and Learning Systems* **30**, 3370–3383 (2019).
- ¹¹S. Siامي-Namini, N. Tavakoli, and A. S. Namin, "The Performance of LSTM and BiLSTM in Forecasting Time Series," in *2019 IEEE International Conference on Big Data (Big Data)* (2019) pp. 3285–3292.
- ¹²Y. Tan, C. Hu, K. Zhang, K. Zheng, E. A. Davis, and J. S. Park, "LSTM-Based Anomaly Detection for Non-Linear Dynamical System," *IEEE Access* **8**, 103301–103308 (2020).
- ¹³Y. Wang, "A new concept using LSTM Neural Networks for dynamic system identification," in *2017 American Control Conference (ACC)* (2017) pp. 5324–5329.
- ¹⁴Y. Huang, L. Yang, and Z. Fu, "Reconstructing coupled time series in climate systems using three kinds of machine-learning methods," *Earth System Dynamics* **11**, 835–853 (2020).
- ¹⁵E. Bollt, "On explaining the surprising success of reservoir computing forecaster of chaos? The universal machine learning dynamical system with contrast to VAR and DMD," *Chaos: An Interdisciplinary Journal of Nonlinear Science* **31**, 013108 (2021).
- ¹⁶Z. Lu, B. R. Hunt, and E. Ott, "Attractor reconstruction by machine learning," *Chaos: An Interdisciplinary Journal of Nonlinear Science* **28**, 061104 (2018).
- ¹⁷J. Pathak, B. Hunt, M. Girvan, Z. Lu, and E. Ott, "Model-Free Prediction of Large Spatiotemporally Chaotic Systems from Data: A Reservoir Computing Approach," *Phys. Rev. Lett.* **120**, 024102 (2018).
- ¹⁸J. Pathak, Z. Lu, B. R. Hunt, M. Girvan, and E. Ott, "Using machine learning to replicate chaotic attractors and calculate Lyapunov exponents from data," *Chaos: An Interdisciplinary Journal of Nonlinear Science* **27**, 121102 (2017).
- ¹⁹P. R. Vlachas, J. Pathak, B. R. Hunt, T. P. Sapsis, M. Girvan, E. Ott, and P. Koumoutsakos, "Backpropagation algorithms and Reservoir Computing in Recurrent Neural Networks for the forecasting of complex spatiotemporal dynamics," *Neural Networks* **126**, 191–217 (2020).
- ²⁰L. Grigoryeva, A. Hart, and J.-P. Ortega, "Learning strange attractors with reservoir systems," *Nonlinearity* **36**, 4674–4708 (2023), arXiv:2108.05024 [cs, eess, math].
- ²¹D. Goswami, "Delay Embedded Echo-State Network: A Predictor for Partially Observed Systems," *IFAC-PapersOnLine 22nd IFAC World Congress*, **56**, 6826–6832 (2023).
- ²²G. A. Gottwald and S. Reich, "Combining machine learning and data assimilation to forecast dynamical systems from noisy partial observations," *Chaos: An Interdisciplinary Journal of Nonlinear Science* **31**, 101103 (2021).
- ²³S. Herzog, R. S. Zimmermann, J. Abele, S. Luther, and U. Parlitz, "Reconstructing Complex Cardiac Excitation Waves From

- Incomplete Data Using Echo State Networks and Convolutional Autoencoders,” *Frontiers in Applied Mathematics and Statistics* **6** (2021).
- ²⁴H. Ribera, S. Shirman, A. V. Nguyen, and N. M. Mangan, “Model selection of chaotic systems from data with hidden variables using sparse data assimilation,” *Chaos: An Interdisciplinary Journal of Nonlinear Science* **32**, 063101 (2022).
- ²⁵S. Shahi, F. H. Fenton, and E. M. Cherry, “Prediction of chaotic time series using recurrent neural networks and reservoir computing techniques: A comparative study,” *Mach Learn Appl* **8**, 100300 (2022).
- ²⁶K. Yeo, “Data-driven reconstruction of nonlinear dynamics from sparse observation,” *Journal of Computational Physics* **395**, 671–689 (2019).
- ²⁷C. D. Young and M. D. Graham, “Deep learning delay coordinate dynamics for chaotic attractors from partial observable data,” *Phys. Rev. E* **107**, 034215 (2023).
- ²⁸L.-W. Kong, Y. Weng, B. Glaz, M. Haile, and Y.-C. Lai, “Digital twins of nonlinear dynamical systems,” (2022), arXiv:2210.06144 [nlin].
- ²⁹N. Trouvain, L. Pedrelli, T. T. Dinh, and X. Hinaut, “ReservoirPy: An Efficient and User-Friendly Library to Design Echo State Networks,” in *Artificial Neural Networks and Machine Learning – ICANN 2020*, Vol. 12397, edited by I. Farkas, P. Masulli, and S. Wermter (Springer International Publishing, Cham, 2020) pp. 494–505.
- ³⁰P. Steiner, A. Jalalvand, S. Stone, and P. Birkholz, “PyRCN: A Toolbox for Exploration and Application of Reservoir Computing Networks,” (2022), arXiv:2103.04807 [cs].
- ³¹T. Akiba, S. Sano, T. Yanase, T. Ohta, and M. Koyama, “Optuna: A Next-generation Hyperparameter Optimization Framework,” (2019), arXiv:1907.10902 [cs, stat].
- ³²J. Bergstra, B. Komer, C. Eliasmith, D. Yamins, and D. D. Cox, “Hyperopt: A Python library for model selection and hyperparameter optimization,” *Comput. Sci. Discov.* **8**, 014008 (2015).
- ³³H. Tamura and G. Tanaka, “Partial-FORCE: A fast and robust online training method for recurrent neural networks,” in *2021 International Joint Conference on Neural Networks (IJCNN)* (2021) pp. 1–8.
- ³⁴D. Sussillo and L. F. Abbott, “Generating Coherent Patterns of Activity from Chaotic Neural Networks,” *Neuron* **63**, 544–557 (2009).
- ³⁵C. Sheng, J. Zhao, W. Wang, and H. Leung, “Prediction Intervals for a Noisy Nonlinear Time Series Based on a Bootstrapping Reservoir Computing Network Ensemble,” *IEEE Transactions on Neural Networks and Learning Systems* **24**, 1036–1048 (2013).
- ³⁶J. Yin and Y. Meng, “Reservoir computing ensembles for multi-object behavior recognition,” in *The 2012 International Joint Conference on Neural Networks (IJCNN)* (2012) pp. 1–8.
- ³⁷S. Ortín and L. Pesquera, “Reservoir Computing with an Ensemble of Time-Delay Reservoirs,” *Cogn Comput* **9**, 327–336 (2017).
- ³⁸D. J. Gauthier, E. Bollt, A. Griffith, and W. A. S. Barbosa, “Next generation reservoir computing,” *Nat Commun* **12**, 5564 (2021).
- ³⁹T. Berry and S. Das, “Learning Theory for Dynamical Systems,” *SIAM J. Appl. Dyn. Syst.* **22**, 2082–2122 (2023).
- ⁴⁰T. L. Carroll, “Low dimensional manifolds in reservoir computers,” *Chaos: An Interdisciplinary Journal of Nonlinear Science* **31**, 043113 (2021).
- ⁴¹T. L. Carroll and L. M. Pecora, “Network structure effects in reservoir computers,” *Chaos: An Interdisciplinary Journal of Nonlinear Science* **29**, 083130 (2019).
- ⁴²X.-Y. Duan, X. Ying, S.-Y. Leng, J. Kurths, W. Lin, and H.-F. Ma, “Embedding theory of reservoir computing and reducing reservoir network using time delays,” *Phys. Rev. Res.* **5**, L022041 (2023).
- ⁴³L. Grigoryeva, A. Hart, and J.-P. Ortega, “Chaos on compact manifolds: Differentiable synchronizations beyond the Takens theorem,” *Phys. Rev. E* **103**, 062204 (2021).
- ⁴⁴A. Hart, J. Hook, and J. Dawes, “Embedding and approximation theorems for echo state networks,” *Neural Networks* **128**, 234–247 (2020).
- ⁴⁵L. Storm, K. Gustavsson, and B. Mehlig, “Constraints on parameter choices for successful time-series prediction with echo-state networks,” *Mach. Learn.: Sci. Technol.* **3**, 045021 (2022).
- ⁴⁶L. A. Thiede and U. Parlitz, “Gradient based hyperparameter optimization in Echo State Networks,” *Neural Networks* **115**, 23–29 (2019).
- ⁴⁷J. Viehweg, K. Worthmann, and P. Mäder, “Parameterizing echo state networks for multi-step time series prediction,” *Neurocomputing* **522**, 214–228 (2023).
- ⁴⁸B. Zhao, “Seeking optimal parameters for achieving a lightweight reservoir computing: A computational endeavor,” *era* **30**, 3004–3018 (2022).